

Supporting Information of

Confining Excitation Energy of Er³⁺-Sensitized Upconversion Nanoparticles through
Introducing Various Energy Trapping Centers

Yunfei Shang,^a Shuwei Hao,^{*a,b} Weiqiang Lv,^c Tong Chen,^a Li Tian,^a Zuotao Lei,^{a,b}
Chunhui Yang^{*a,b,d}

a MIIT Key Laboratory of Critical Materials Technology for New Energy Conversion and Storage, School of Chemistry and Chemical Engineering, Harbin Institute of Technology, Harbin 150001, China. *Email - yangchh@hit.edu.cn

b Key Laboratory of Micro-systems and Micro-structures Manufacturing of Ministry of Education, Harbin Institute of Technology

c School of Physics, University of Electronic Science and Technology, Chengdu, Sichuan 611731, China

d State Key Laboratory of Urban Water Resource and Environment, Harbin Institute of Technology

Experimental section

Materials:

All chemicals were of analytical grade and used without further purification. $\text{ErCl}_3 \cdot 6\text{H}_2\text{O}$ (99.99%), $\text{YCl}_3 \cdot 6\text{H}_2\text{O}$ (99.99%), $\text{TmCl}_3 \cdot 6\text{H}_2\text{O}$ (99.99%), $\text{YbCl}_3 \cdot 6\text{H}_2\text{O}$ (99.99%), $\text{NdCl}_3 \cdot 6\text{H}_2\text{O}$ (99.99%), $\text{HoCl}_3 \cdot 6\text{H}_2\text{O}$ (99.99%), $\text{PrCl}_3 \cdot 6\text{H}_2\text{O}$ (99.99%), $\text{EuCl}_3 \cdot 6\text{H}_2\text{O}$ (99.99%), $\text{CeCl}_3 \cdot 6\text{H}_2\text{O}$ (99.99%) were supplied by Beijing Founde Star Science and Technology Co., Ltd China. NaOH (99%), NH_4F (99%), cyclohexane (99.9%), 1-octadecene (ODE, 90%), oleic acid (OA, AR) were obtained from Aladdin. Chloroplatinic acid hexahydrate (H_2PtCl_6 , ACS reagent), ethanol (ACS reagent, absolute), ethyl cellulose (EC), terpineol and N719 dye were purchased from the Aladdin. Fluorine-doped tin oxide (FTO) conducting glass plates (sheet resistance $10 \Omega \text{ sq}^{-1}$) and P_{25} (TiO_2) were purchased from Qiseguang Technology Ltd. in China.

Synthesis of $\beta\text{-NaYF}_4:x\%\text{Er}^{3+}$ core nanoparticles:

The oleic-acid-capped core nanoparticles ($\beta\text{-NaYF}_4:x\%\text{Er}^{3+}$) were synthesized by a solvothermal method adapted from our recent work¹. A typical procedure is as follows: $\text{YCl}_3 \cdot 6\text{H}_2\text{O}$ ($1-x$ mmol) and $\text{ErCl}_3 \cdot 6\text{H}_2\text{O}$ (x mmol) were added into a 100 mL three-necked flask containing 6 mL oleic acid (OA) and 15 mL 1-octadecene (ODE). The mixture was first heated to 160 °C to form a transparent solution and remove residual water, and then cooled down to room temperature. 10 mL of methanol solution containing NaOH (2.5 mmol) and NH_4F (4 mmol) was slowly dropped into the flask and stirred for 30 min. Then the solution was heated to 70-80 °C and maintained for 30 min to evaporate methanol. Subsequently, the solution was heated to 310 °C and

maintained for 1 h under argon atmosphere. After cooling down to room temperature, the resulting products were precipitated by ethanol and collected by centrifugation at 6000 rpm for 5 min. The precipitate was then purified with ethanol three times, and finally dispersed in 10ml cyclohexane for further use.

Synthesis of β -NaYF₄:x%Er³⁺@ β -NaYF₄ core@shell nanoparticles:

In a typical experiment, a 100 mL three-necked flask containing 6 mL oleic acid (OA) and 15 mL 1-octadecene (ODE) were added given amounts of YCl₃·6H₂O (0.50 mmol) and the NaYF₄:x%Er³⁺ core (1 mmol) in cyclohexane were also added after then. The mixture was heated to 160 °C to form a transparent solution and remove residual water and cyclohexane, and then cooled down to room temperature. 5 mL of methanol solution containing NaOH (1.25 mmol) and NH₄F (2 mmol) was slowly dropped into the flask and stirred for 30 min to ensure that all fluoride was completely consumed. Then the solution was then heated to 70-80 °C for evaporating methanol completely from the reaction mixture. Subsequently, the solution was heated to 31°C and maintained for 1 h under argon atmosphere. After cooling down to room temperature, the resulting products were precipitated by ethanol and collected by centrifugation at 6000 rpm for 5 min. The precipitate was then purified with ethanol three times, and finally dispersed in cyclohexane for further measurement.

Fabrication of Dye-sensitized Solar Cells¹:

Transparent fluorine-doped tin oxide (FTO) glass was used as substrate. FTO was sequentially cleaned in absolute ethanol, and deionized (DI) water for 15 min under ultrasonic treatment, then the cleaned FTO was dried at 80 °C for further use. 1.00 g EC powder was dissolved in 50 ml absolute ethanol, and mixed with 2.0g P₂₅ (TiO₂)

nanoparticles suspension, followed by sonication for 30 min at room temperature. Terpineol (8.69 ml) was added dropwise into the as-prepared mixture. Subsequently, the ethanol in the mixture was removed on a rotary evaporator at 65°C for 2 hours. Then, the TiO₂ films were screen-printed on FTO substrate, followed by being sintered at 450°C for 1 h and 500°C for 30 min in nitrogen. The sintered film was post-treated in a fresh aqueous TiCl₄ solution (30 mM) at 70 °C for 30min. Then, the TiO₂ film treated by TiCl₄ was sintered at 500°C for 30min. After that, UCNPs were deposited onto the TiO₂ film simply by immersing the films into UCNPs solution (0.01 M) in cyclohexane for 10 min. Subsequently, the UCNPs coated TiO₂ film was sintered at 100°C for 30min. After cooling down to 80 °C, the sintered photoanodes were immersed in 0.5 mM N719 dye in acetonitrile/tert-butanol mixed solution (1:1, v/v) for 24 h. The platinized counter electrodes were prepared by thermal deposition of H₂PtCl₆ solution (10 mM in isopropanol) onto FTO glass at 450°C for 30 min.

TiO₂ films photoanode and platinized counter electrode were sealed with a 25µm thick Surlyn at 90°C. There is a reserved hole in the counter electrode, where electrolyte can be introduced into the solar cells. The hole was finally sealed with a Surlyn and a thin glass. Under each condition, at least three samples were prepared for the measurements in order to obtain a medium value as the final data.

Characterizations

Transmission Electron Microscopy:

The morphology and size of the resulting nanoparticles were investigated by means of transmission electron microscope (TEM, Tecnai G2 Spirit Twin 12) operating at 80 kV. High resolution transmission electron microscopic (HRTEM) images were obtained on the microscope of Spirit Twin Tecnai G2 D339 operating at 300 kV.

X-ray Diffraction:

The powder X-Ray diffraction (XRD) pattern was carried out on a Rigaku D/max- γ B diffractometer equipped with a rotating anode and a Cu K α source ($\lambda=0.15418$ nm). The 2θ angle of the XRD spectra was recorded at a scanning rate of $5^\circ/\text{min}$ from 20° to 80° .

Upconversion Spectra:

Upconversion spectra were recorded using a lens-coupled monochromator (Zolix Instruments Co. Ltd., Beijing, China) with a slit width defining spectral resolution of 2 nm. The emissions were excited at 980 nm and 1532 nm using a fiber-coupled laser diode (Hi-Tech Optoelectronics Co. Ltd., Beijing). Decay profiles were measured using square-wave modulated direct current, and then recorded by Tektronix MDO 3024 mixed Domain oscilloscope coupled with the photo multiplied tube (PMT), using excitation at 980 nm from laser diode (Q-Photonics) operating in pulsed mode.

Study of excitation power density dependence of upconversion emission:

Measurement of power density dependence on upconversion luminescence was conducted to study the multi-photon-pumped upconversion process. Typically, upconversion luminescence intensity I_{UC} is n power of the excitation power density I_P :

$$I_{UC} \propto I_P^n$$

Where n denotes the number of the photons for upconversion population.

Current density–voltage (J – V) and IPCE characteristics:

The current density-voltage (J - V) characteristics were measured by using a computerized Keithley 2400 source meter. Sun simulator (Oriel, AM 1.5G illumination at 100 mW/cm²) was used as light sources. A black mask (6 × 6 mm) was used in the subsequent photovoltaic studies. The incident photon to current efficiency (IPCE) spectra were measured using a tungstenhalogen light source combined with a monochromator (Spectra Pro 2300, Acton Research), and a lock-in amplifier (SR-830, Stanford Research) by locking to the modulation frequency.

The effective lifetime formula of the electron in the oxide film ^{2,3}

$$\tau_r = \frac{1}{\omega_{max}} = \frac{1}{2\pi f_{max}}$$

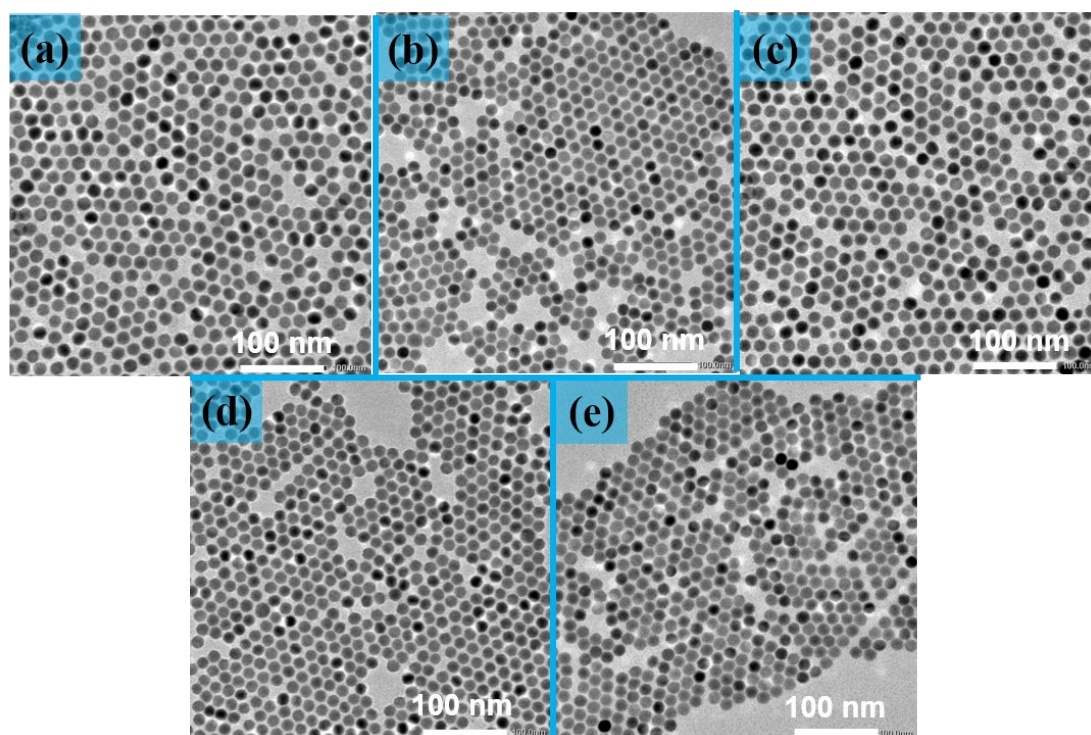


Fig. S1 Structure characterization of $\text{NaYF}_4:x \text{ mol \%Er}^{3+}$ bare core nanoparticles. The low-resolution transmission electron microscopy (TEM) images of (a) $\text{NaYF}_4:10\%\text{Er}^{3+}$, (b) $\text{NaYF}_4:20\%\text{Er}^{3+}$, (c) $\text{NaYF}_4:50\%\text{Er}^{3+}$, (d) $\text{NaYF}_4:70\%\text{Er}^{3+}$, (e) NaErF_4 . These results show that this synthetic route can be used for producing high-quality UCNPs with uniform size. Moreover, the increasing of Er^{3+} content from 10% to 100% in NaYF_4 lattice has no effect on the morphology and size of UCNPs.

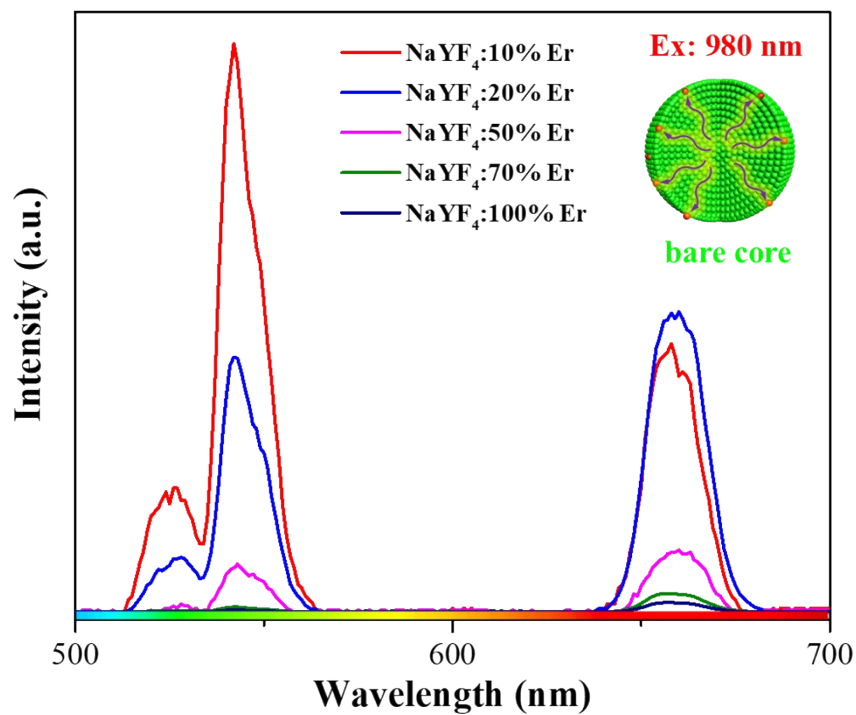


Fig. S2 Upconversion emission spectra of the bare core nanoparticles with variable Er³⁺ dopant concentrations under 980 nm CW laser diode excitation. With the increase of Er³⁺ doping concentrations, the rapid decline of luminescence intensity is aroused from Er³⁺ concentration quenching.

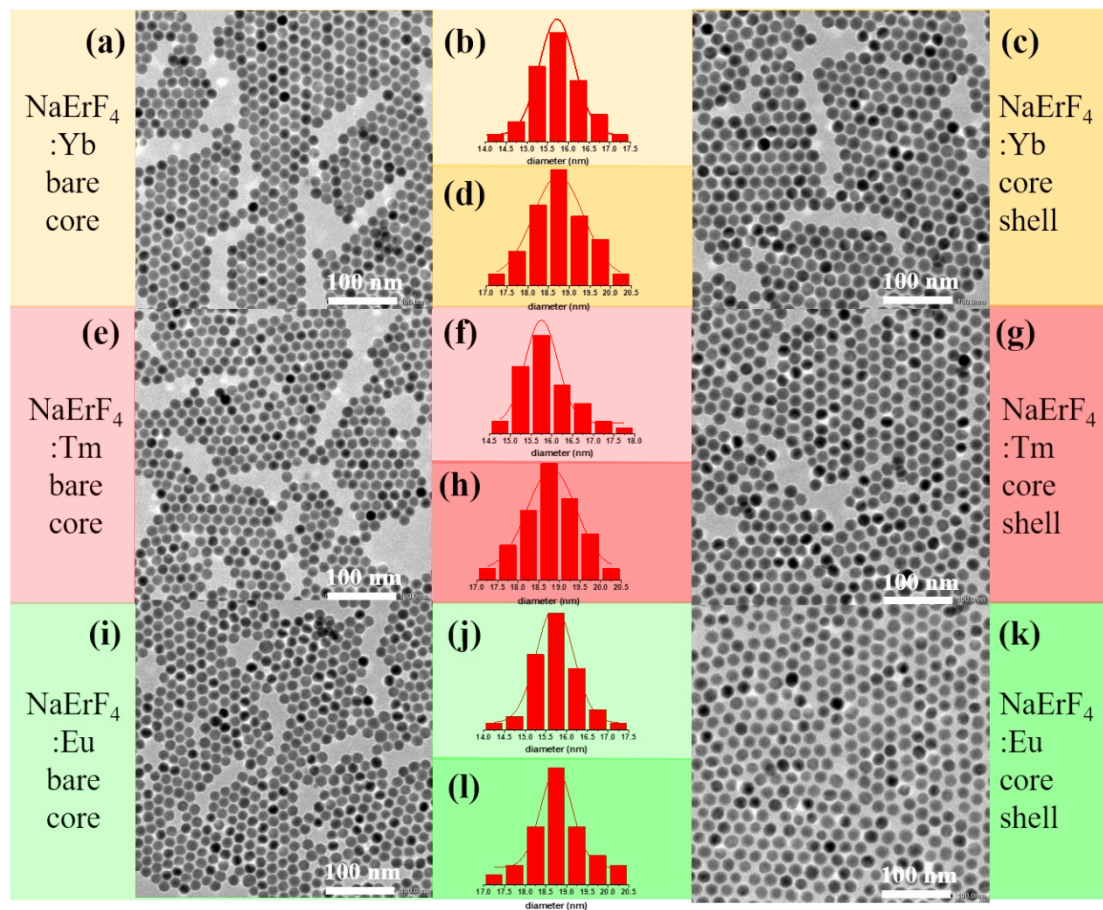


Fig. S3 Structure characterization of $\text{NaErF}_4:\text{Ln}^{3+}$ bare core and core-shell (~ 1.5 nm) nanoparticles. The low-resolution transmission electron microscopy (TEM) images and nanoparticle size distribution of (a) (b) $\text{NaErF}_4:10\%\text{Yb}^{3+}$, (c) (d) $\text{NaErF}_4:10\%\text{Yb}^{3+}@\text{NaYF}_4$, (e) (f) $\text{NaErF}_4:0.5\%\text{Tm}^{3+}$, (g) (h) $\text{NaErF}_4:0.5\%\text{Tm}^{3+}@\text{NaYF}_4$, (i) (j) $\text{NaErF}_4:0.5\%\text{Eu}^{3+}$, (k) (l) $\text{NaErF}_4:0.5\%\text{Eu}^{3+}@\text{NaYF}_4$. Scale bar in each TEM image is 100 nm. The sizes of UCNPs doped with various trapping centers increased from 15.7nm to 18.7nm after coating a NaYF_4 layer, confirming the formation of core/shell structure with a 3nm shell layer.

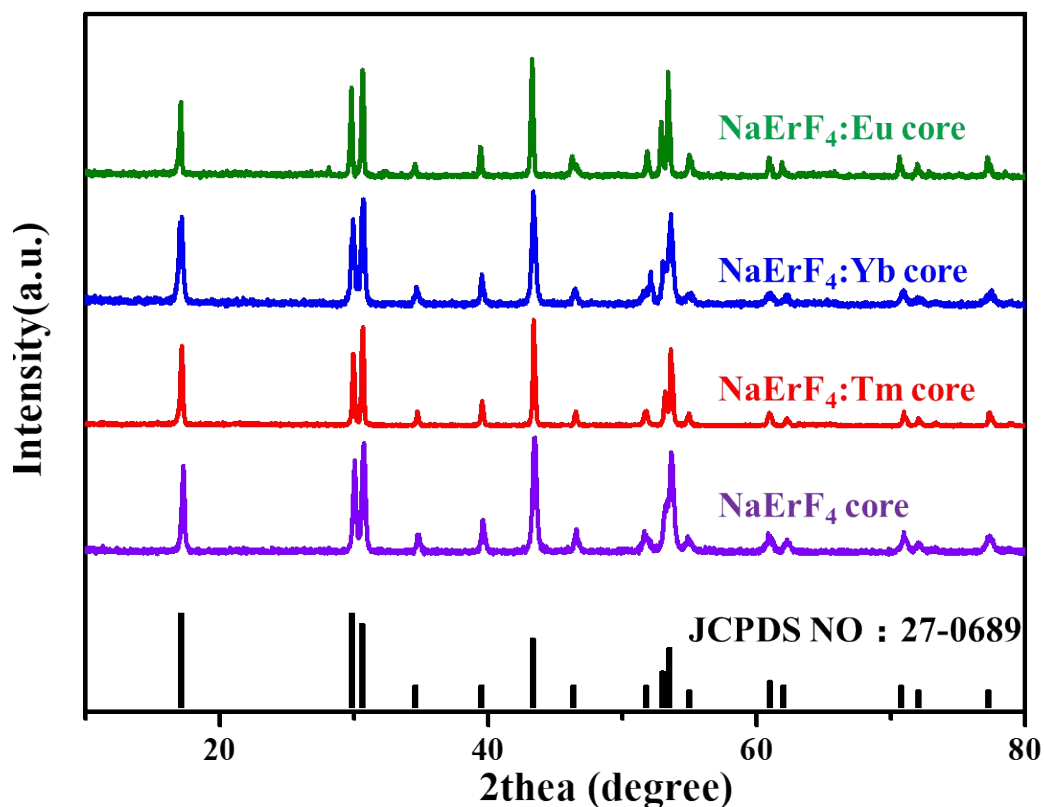


Fig. S4 Corresponding powder XRD diffraction patterns of the NaErF₄, NaErF₄:0.5%Tm³⁺, NaErF₄:10%Yb³⁺ and NaErF₄:0.5%Eu³⁺ bare core nanoparticles.

The standard pattern JCPDS No. 27-0689 of hexagonal phase NaErF₄ host material is included as a reference. These results confirm various rare-earth ions serving as energy trapping centers were successfully introduced into NaErF₄ lattice.

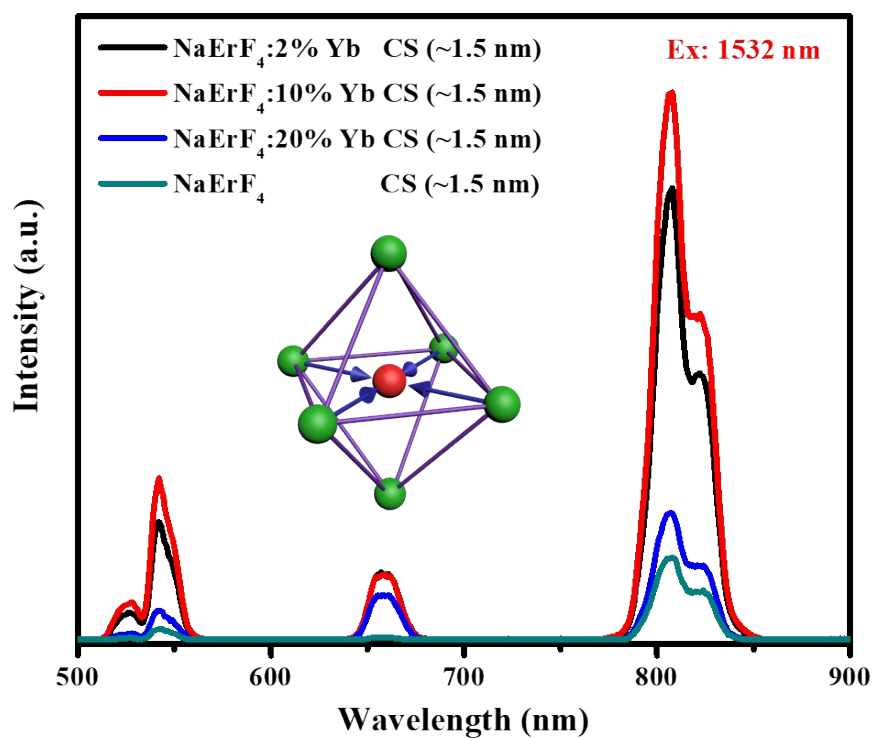


Fig. S5 Upconversion emission spectra of the NaErF₄:Yb³⁺@NaYF₄ core-shell (~1.5 nm) nanoparticles with variable Yb³⁺ dopant concentrations (0%, 2%, 10%, 20%) under 1532 nm CW laser diode excitation. The upconverting luminescence of the optimized NaErF₄:Yb³⁺@NaYF₄ core/shell nanoparticles generated a great enhancement of emitting intensity, illustrating the highly efficient excitation energy confinement of the optimal 10% Yb trapping centers.

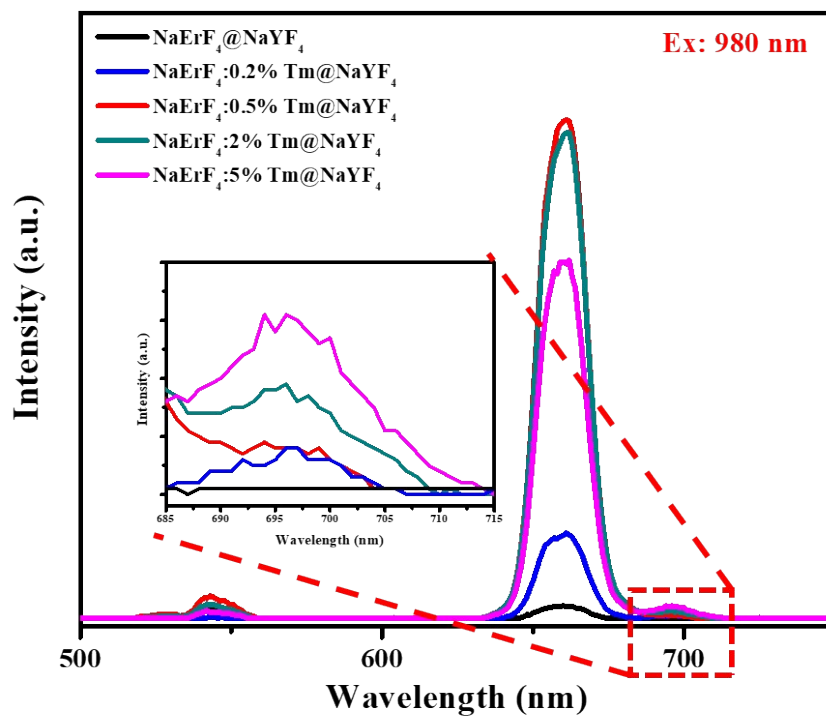


Fig. S6 Upconversion emission spectra of the NaErF₄:Tm³⁺@NaYF₄ core-shell (~1.5 nm) nanoparticles with variable Tm³⁺ dopant concentrations under 980 nm CW laser diode excitation. Note that 0.5 mol% is the best doping concentration for Tm³⁺.

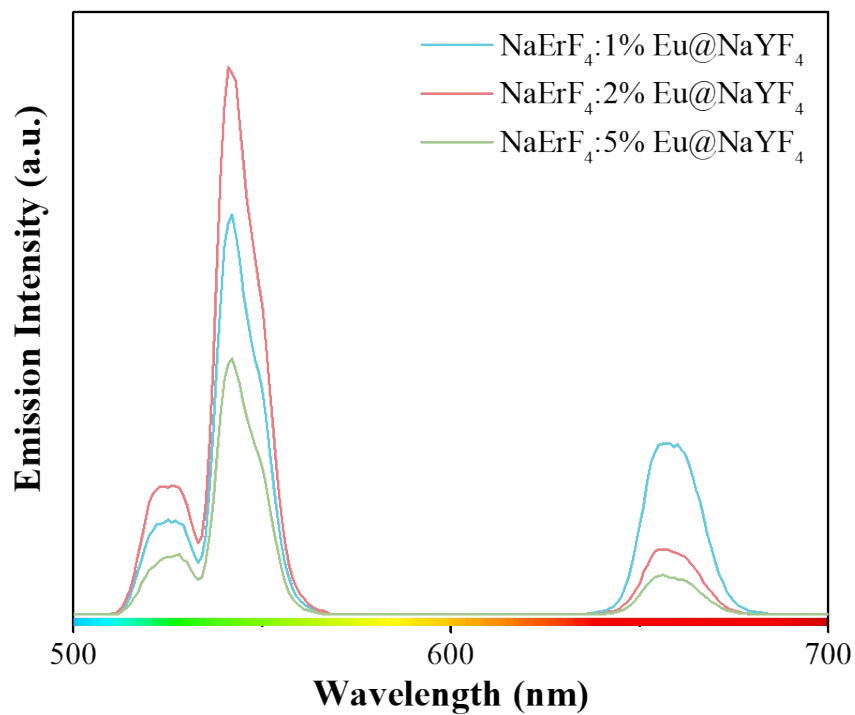


Fig. S7 Upconversion emission spectra of the NaErF₄:Eu³⁺@NaYF₄ core-shell (~1.5 nm) nanoparticles with variable Eu³⁺ dopant concentrations under 980 nm CW laser diode excitation. The result shows that the optimal doping concentration of Eu³⁺ trapping center in NaErF₄@NaYF₄ core-shell structure is 2%.

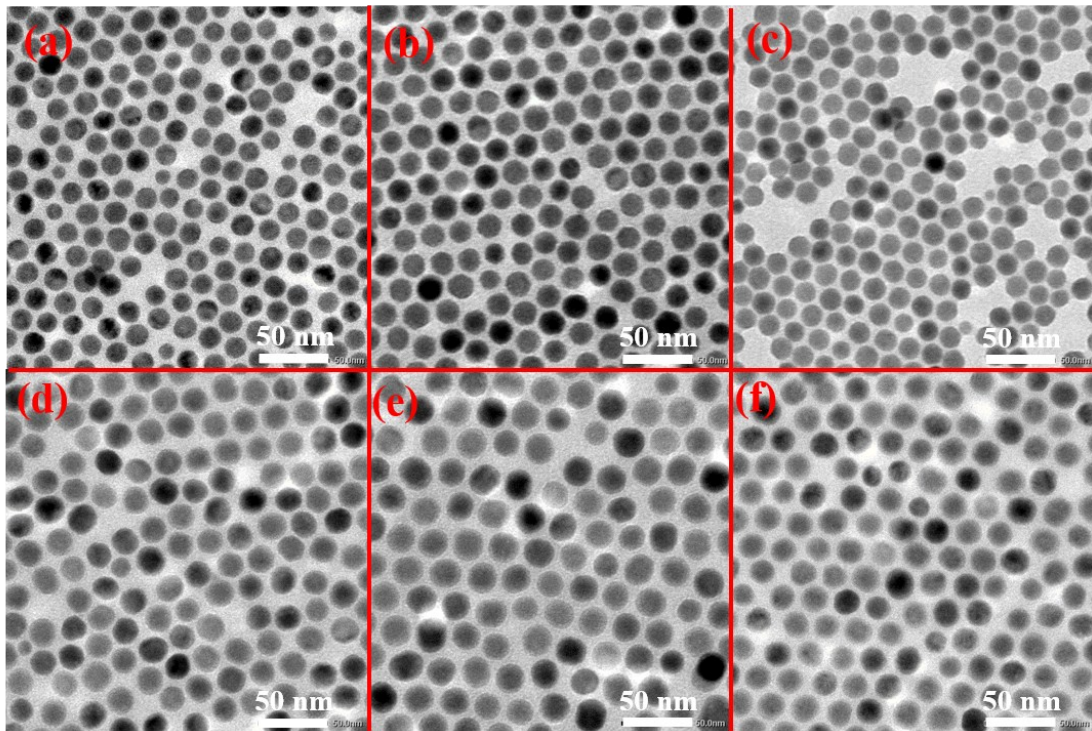


Fig. S8 Structure characterization of $\text{NaErF}_4:\text{Ln}^{3+}$ bare core and core-shell (~ 1.5 nm) nanoparticles. The low-resolution transmission electron microscopy (TEM) images of (a) $\text{NaErF}_4:\text{Ho}^{3+}$, (b) $\text{NaErF}_4:\text{Pr}^{3+}$, (c) $\text{NaErF}_4:\text{Ce}^{3+}$, (d) $\text{NaErF}_4:\text{Ho}^{3+}@\text{NaYF}_4$, (e) $\text{NaErF}_4:\text{Pr}^{3+}@\text{NaYF}_4$, (f) $\text{NaErF}_4:\text{Ce}^{3+}@\text{NaYF}_4$, Scale bar in each TEM image is 50 nm. These results confirm that the morphologies and sizes of doped UCNPs were not affected by the doping of rare-earth ions serving as energy trapping centers.

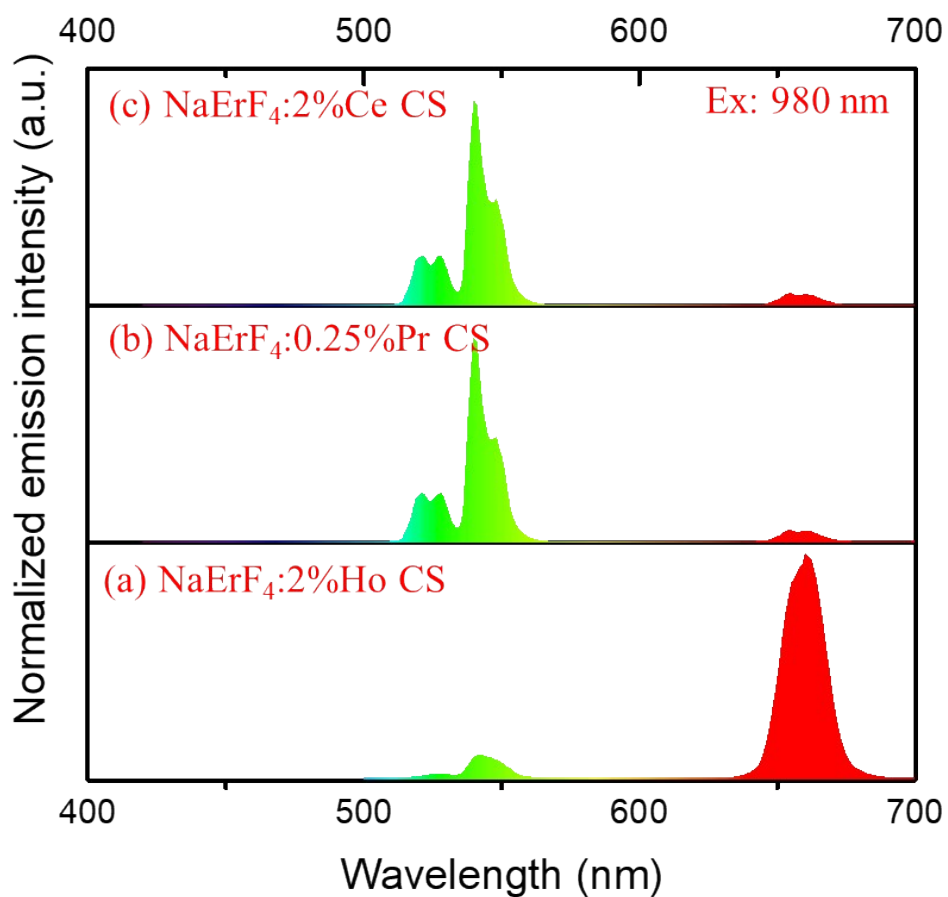


Fig. S9 Normalized upconversion emission spectra of (a) NaErF₄:Ho³⁺@NaYF₄, (b) NaErF₄:Pr³⁺@NaYF₄ and (c) NaErF₄:Ce³⁺@NaYF₄. These results indicate that the Ce and Pr trapping centers are beneficial for tuning the green emission of NaErF₄@NaYF₄ nanoparticles, however, the Ho trapping center is conducive to increase the red output of NaErF₄@NaYF₄ nanoparticles.

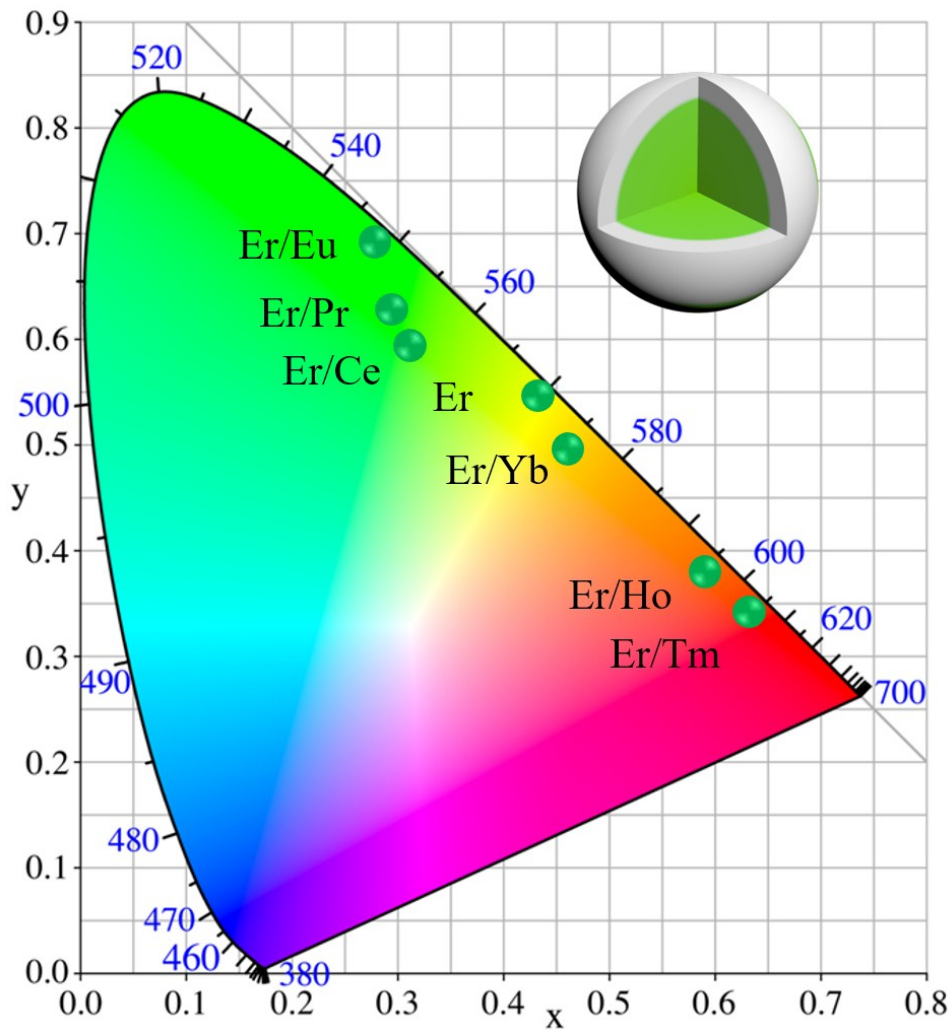


Fig. S10 Corresponding Commission Internationale de l'Eclairage (CIE) chromaticity coordinates of the multicolour emissions from the samples co-doped with Yb^{3+} , Tm^{3+} , Eu^{3+} , Ho^{3+} , Pr^{3+} and Ce^{3+} , *et al.* in $\text{NaErF}_4@ \text{NaYF}_4$ core-thin shell structure. The calculated chromaticity coordinates clearly indicate the tuning trend of UC luminescence color from red to green in $\text{NaErF}_4@ \text{NaYF}_4$ system through changing the types of energy trapping centers.

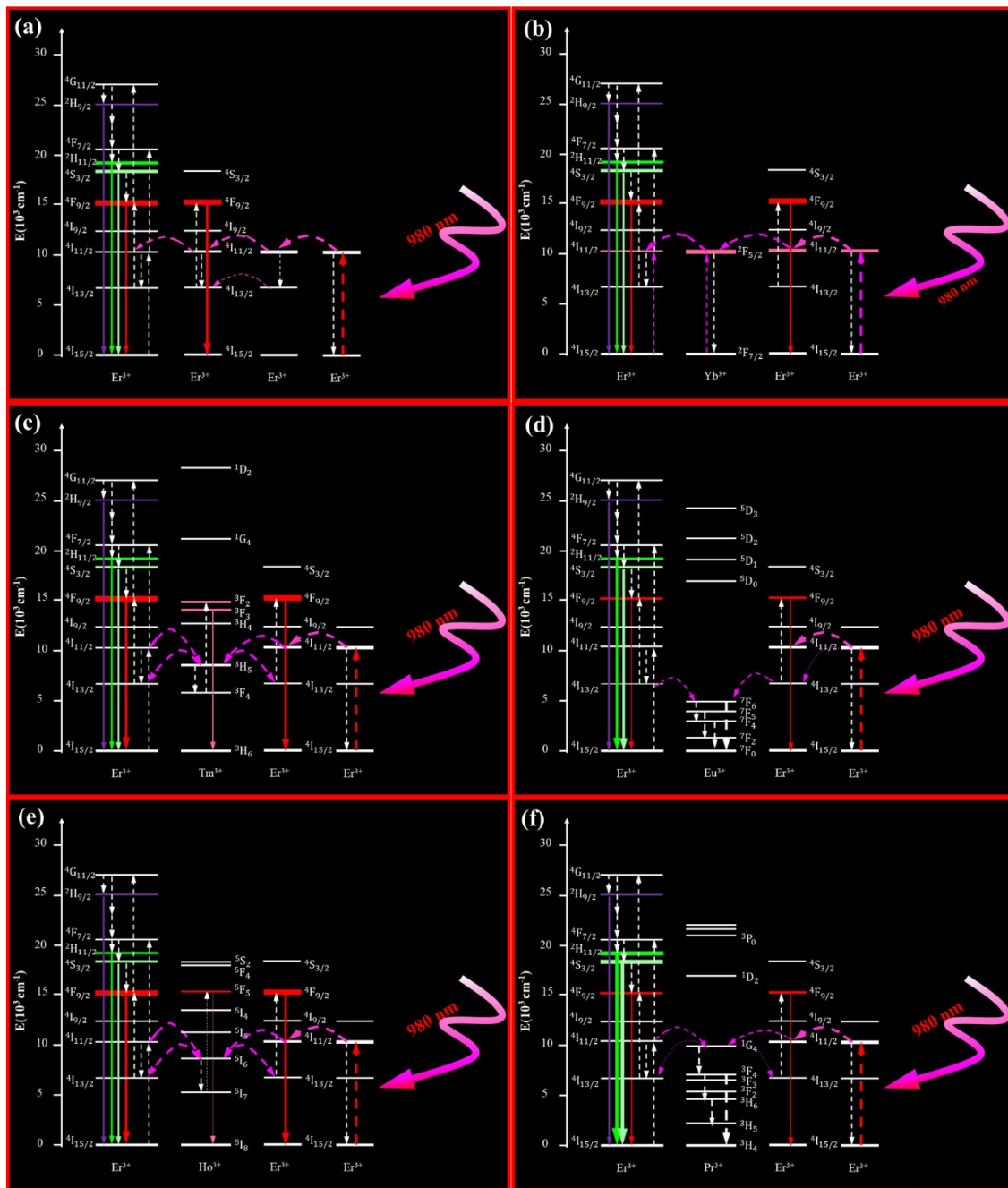


Fig. S11 Simplified energy level diagram and proposed mechanism for UC processes of 980 nm photons in (a) β -NaErF₄@NaYF₄, (b) β -NaErF₄:Yb@NaYF₄, (c) β -NaErF₄:Tm@NaYF₄, (d) β -NaErF₄:Eu@NaYF₄, (e) β -NaErF₄:Ho@NaYF₄, (f) β -NaErF₄:Pr@NaYF₄

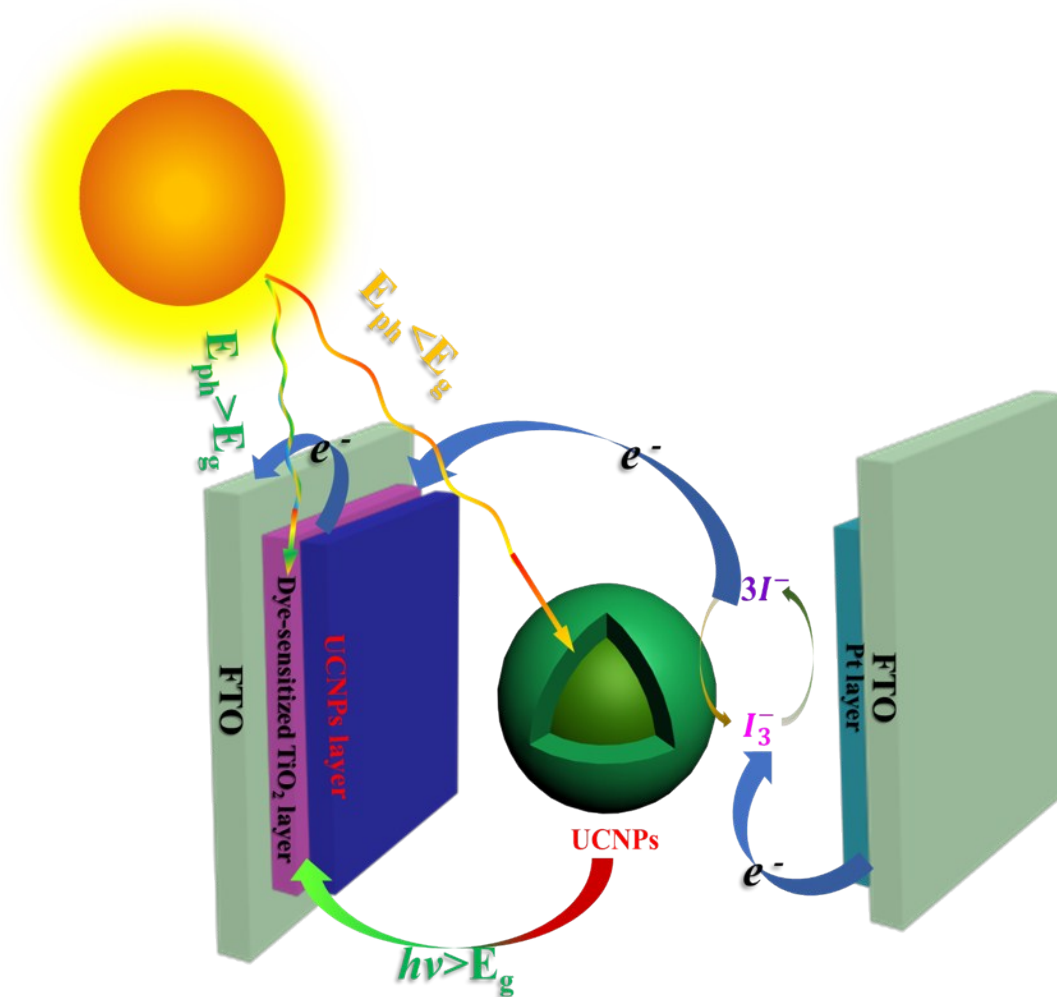


Fig. S12 Schematic illustration of proposed working principle of the upconversion induced photoelectrode in DSSCs. The left part of Fig. S12 portrays the configuration of a DSSC structure where UCNPs doped with energy trapping centers are placed on top of the mesoporous TiO₂ layer. The light-absorbing dyes (N719) in regular DSSC devices (without involving UCNPs) is only able to harvest ultraviolet-visible spectral range (350–670 nm) of standard AM1.5 sunlight, with radically reduced absorption capability at the edge of longer wavelength absorption. An introduction of UCNPs into the DSSC device enables capturing NIR photons in a new and multiband spectral range of 1532 nm, 980 nm and 800 nm (due to the absorption of Er³⁺), and then the absorbed

NIR photons can be upconverted to 540/650 nm luminescence that matches the absorption spectrum of the N719 dye. In this way, the harvested NIR energy is upconverted to activate the N719 dye to produce charge carriers, improving the photovoltaic performance of a DSSC device.

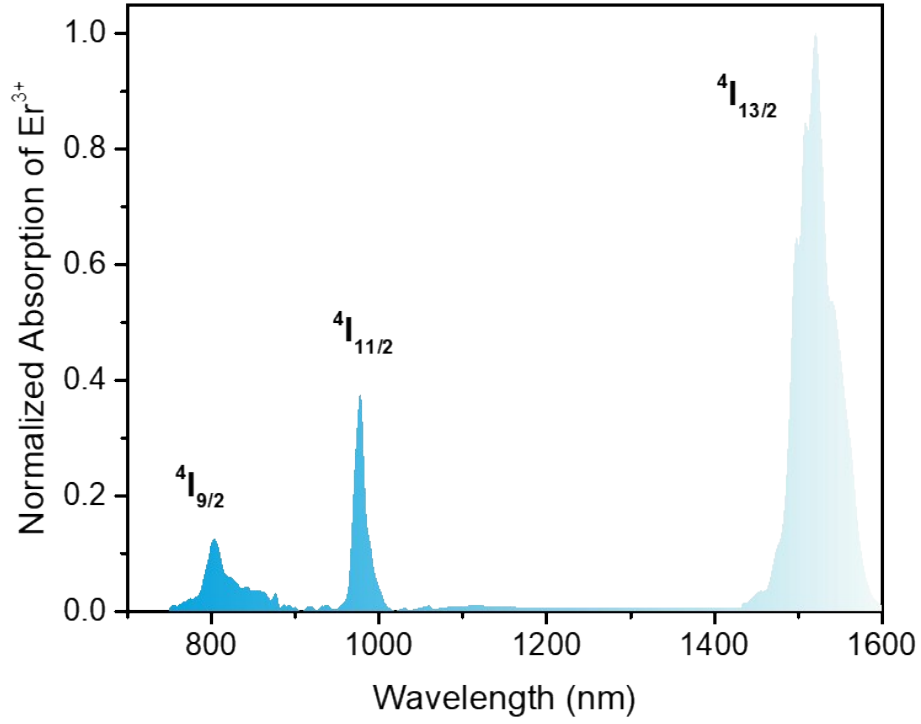


Fig. S13 Normalized absorption spectrum of as-prepared NaErF₄: 10Yb@NaYF₄ nanoparticles in cyclohexane. This result confirms that NaErF₄:10Yb@NaYF₄ nanoparticles is able to simultaneously harvest multiband NIR photons with the peaks located at 1532 nm, 980nm and 800nm.

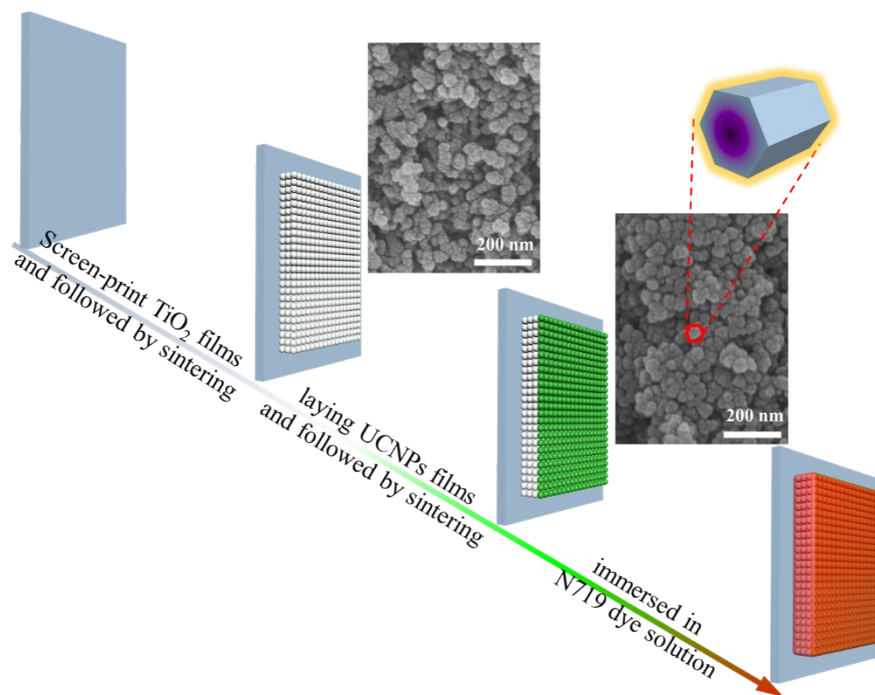


Fig. S14 Schematic illustration of the preparation process of photoanode treated with Er^{3+} -sensitized core@shell UCNPs. And the insets are the typical Field emission scanning electron microscopy (FESEM) images of the TiO_2 photoanodes before and after treated with $\text{NaErF}_4@\text{NaYF}_4$ nanoparticles.

Reference

1. S. W. Hao, Y. F. Shang, D. Y. Li, H. Agren, C. H. Yang and G. Y. Chen, *Nanoscale*, 2017, **9**, 6711-6715.
2. J. Chen, J. Wu, W. Lei, J. L. Song, W. Q. Deng and X. W. Sun, *Appl Surf Sci*, 2010, **256**, 7438-7441.
3. A. Subramanian, J. S. Bow and H. W. Wang, *Thin Solid Films*, 2012, **520**, 7011-7017.